

RSC Advances



This is an *Accepted Manuscript*, which has been through the Royal Society of Chemistry peer review process and has been accepted for publication.

Accepted Manuscripts are published online shortly after acceptance, before technical editing, formatting and proof reading. Using this free service, authors can make their results available to the community, in citable form, before we publish the edited article. This *Accepted Manuscript* will be replaced by the edited, formatted and paginated article as soon as this is available.

You can find more information about *Accepted Manuscripts* in the [Information for Authors](#).

Please note that technical editing may introduce minor changes to the text and/or graphics, which may alter content. The journal's standard [Terms & Conditions](#) and the [Ethical guidelines](#) still apply. In no event shall the Royal Society of Chemistry be held responsible for any errors or omissions in this *Accepted Manuscript* or any consequences arising from the use of any information it contains.

Cite this: DOI: 10.1039/c0xx00000x

www.rsc.org/xxxxxx

ARTICLE TYPE

A triphenylamine-based colorimetric and “turn-on” fluorescent probe for live-cell detection of cyanide anion

Shaodan Wang,^a Hai Xu,^a Qingbiao Yang,^{*a} Yan Song,^{*b} and Yaoxian Li^a

Received (in XXX, XXX) Xth XXXXXXXXX 20XX, Accepted Xth XXXXXXXXX 20XX

DOI: 10.1039/b000000x

A new colorimetric and “turn-on” fluorescent probe was developed for detection of cyanide anion. The detection of cyanide was performed via the nucleophilic addition of cyanide to the indolium group of the probe, resulting in a huge color change from purple to colorless and the fluorescence enhancement. The probe showed high sensitivity and selectivity for cyanide over other common anion species in aqueous ethanol solution. The limit of detection was found to be as low as 21 nM. In addition, the live cell imaging experiment demonstrated the practical value of the probe in tracing CN⁻ in biological systems.

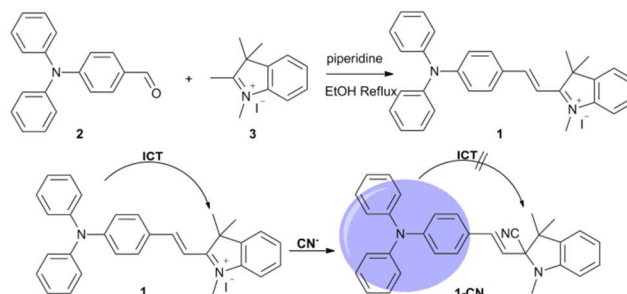
1. Introduction

Anions recognition chemistry has received considerable attention in the past decades due to their important role in a wide range of biological, environmental and chemical applications.¹ Among various anions, cyanide anion (CN⁻) is widely utilized in many industrial processes, including gold mining, electroplating, metallurgy and resins industry.² However, it is extremely toxic and can lead to many functions in human body, such as vomiting, convulsion, loss of consciousness, and eventual death.³ According to the World Health Organization (WHO), the maximum permissible level of cyanide in drinking water is only 1.9 μM.⁴ Therefore, it is highly desirable to find an efficient way for sensitive and selective detection of cyanide anions.

Various conventional methods, which are based on spectrophotometric,⁵ electrochemical,⁶ voltammetric,⁷ titrimetric⁸ and other techniques,⁹ have been developed for its quantitative analysis. However, as a consequence of their often complex and time consuming nature and their reliance on instrumentation, the utilization of these methods is limited. Recently, a number of promising fluorescent probes and organic dyes have been constructed as optical sensors for cyanide anions.¹⁰ Among them, several sensor systems have been reported, involving utilization of the coordination of cyanide anion with metal ion,¹¹ hydrogen-bonding interactions,¹² boronic acid derivatives,¹³ deprotonation,¹⁴ and so on. What's more, the nucleophilic addition reactions of cyanide were applied for sensing of cyanide, including reactions with oxazine,¹⁵ pyrylium,¹⁶ indolium,¹⁷ pyridinium,¹⁸ acridinium,¹⁹ dicyano-vinyl group,²⁰ salicylaldehyde,²¹ trifluoroacetamide derivatives,²² and other highly electron deficient carbonyl groups.²³ Despite their simple, inexpensive, and convenient implementation, drawbacks still exist for most sensors. Such as some of them just show high detection limits or generally display moderate selectivity over other anions,²⁴ and the fact that the detection of cyanide cannot be performed in aqueous solution in some cases.²⁵ Therefore,

colorimetric and fluorescent probes for cyanide anion in aqueous solution,²⁶ in particular, with high detection level and high selectivity, are still in great need.

In this regard, we report a new fluorescent turn-on probe for detection of CN⁻ in aqueous ethanol solution based on triphenylamine-hemicyanine dye (shown in Scheme 1). As its indolium 2-C atom is an effective target for nucleophilic addition, the cyanide anions can easily combine with it, thus, interrupts the conjugation between indolium and aldehyde resulting in spectroscopy changes.²⁷ Upon addition of cyanide, the color of solution changed from purple to colorless accompanied with the increase in fluorescence, which achieved dual-channel sensing of cyanide anion. Importantly, probe **1** displayed lower limit of detection²⁸ and higher selectivity²⁹ than some reported probes.



Scheme 1. Synthetic procedure and proposed cyanide-sensing mechanism of probe 1.

2. Experimental section

2.1 Materials and Instruments

1,2,3,3-tetramethyl-3H-indolium iodide, tetrabutylammonium salts were purchased from Sigma–Aldrich and used without further purification. 4-(diphenylamino)benzaldehyde (compound **2**) was prepared according the reported procedure.³⁰ Reagents with analytical grades and deionized water were used for preparing the solutions. Stock solutions of CN⁻, F⁻, Cl⁻, Br⁻, I⁻,

were prepared from their tetrabutylammonium salts; NO_3^- , HSO_3^- , SCN^- , HPO_4^{2-} , H_2PO_4^- , AcO^- , SO_4^{2-} , HS^- , N_3^- were prepared by direct dissolution of proper amounts of sodium salts. Aqueous Tris-HCl buffer (pH = 7.4, 10.0 mM) solution was used as buffer

to keep pH value of testing system.

^1H NMR and ^{13}C NMR spectra were measured on a Bruker AV-400 spectrometer. Absorption and fluorescence spectra were carried out on a Shimadzu UV 2100 PC UV-visible spectrophotometer and a Hitachi F-4500 fluorescence spectrometer, respectively. The pH values of the test solutions were measured with a glass electrode connected to a Mettler-Toledo Instrument DELTA 320 pH meter (Shanghai, China) and adjusted if necessary. All the measurement experiments were performed at room temperature.

2.2 Synthesis

2.2.1 Synthesis of (E)-2-(4-(diphenylamino)styryl)-1,3,3-trimethyl-3H-indol-1-ium iodide (probe 1)

Probe **1** was conveniently prepared via the condensation of 4-(diphenylamino)benzaldehyde (**2**) with 1,2,3,3-tetramethyl-3H-indolium iodide (**3**) in ethanol. Compound **2** (0.828 g, 3.0 mmol) and compound **3** (0.903 g, 3.0 mmol), piperidine (0.3 ml, 3 mmol) were dissolved in 30 ml ethanol. The reaction mixture was refluxed with stirring for 12 h under nitrogen. After cooling the solid was collected, washed with anhydrous ethanol, and then dried. The residue was purified by column chromatography on silica gel ($\text{CH}_2\text{Cl}_2/\text{ethanol}$, 20:1 v/v) to give **1** as a dark purple solid (1.25 g, Yield: 72.2%); ^1H NMR (400 MHz, CDCl_3) δ 8.04 (dd, $J = 18.8, 12.1$ Hz, 3H), 7.62 (d, $J = 15.8$ Hz, 1H), 7.58 – 7.44 (m, 1H), 7.38 (t, $J = 7.4$ Hz, 4H), 7.26 (d, $J = 4.6$ Hz, 2H), 7.20 (d, $J = 7.7$ Hz, 4H), 7.01 (d, $J = 8.4$ Hz, 2H), 4.34 (s, 3H), 1.81 (s, 6H); ^{13}C NMR (101 MHz, DMSO) δ 181.27, 153.40, 152.71, 145.66, 143.61, 142.35, 133.42, 130.60, 129.34, 129.05, 126.92, 126.35, 123.28, 118.89, 114.99, 109.49, 52.06, 40.64, 40.43, 40.22, 40.02, 39.81, 39.60, 39.40, 34.54, 26.24; HRMS (positive mode, m/z): Calcd. 429.2325, found 429.5428 for $[\text{M}+\text{H}]^+$.

2.2.2 Synthesis of (E)-2-(4-(diphenylamino)styryl)-1,3,3-trimethylindoline-2-carbonitrile (1-CN)

The **1-CN** product could be conveniently synthesized via the condensation of **1** and 1.5 equiv. of $(\text{CH}_3\text{CH}_2\text{CH}_2\text{CH}_2)_4\text{N}(\text{CN})$ in ethanol at room temperature, and purified by column chromatography on silica gel (CH_2Cl_2) (yield: 80%). Note: the product is very unstable, and will decompose when exposed in the air. ^1H NMR (400 MHz, CDCl_3) δ 7.34 (d, $J = 7.8$ Hz, 2H), 7.27 (t, $J = 7.4$ Hz, 4H), 7.17 (t, $J = 7.6$ Hz, 1H), 7.11 (d, $J = 7.7$ Hz, 4H), 7.06 (d, $J = 5.4$ Hz, 6H), 6.85 (t, $J = 7.3$ Hz, 1H), 6.59 (d, $J = 7.8$ Hz, 1H), 6.09 (d, $J = 16.1$ Hz, 1H), 2.78 (s, 3H), 1.53 (s, 3H), 1.19 (s, 3H); ^{13}C NMR (101 MHz, CDCl_3) δ 148.68, 148.47, 147.35, 136.68, 135.65, 129.42, 129.06, 128.31, 127.90, 124.78, 123.44, 123.08, 121.81, 120.59, 120.31, 117.53, 108.89, 80.59, 77.40, 77.08, 76.76, 53.48, 49.14, 31.63, 24.56, 22.98; HRMS (positive mode, m/z): Calcd. 455.2361, found 456.2174 for $[\text{M}+\text{H}]^+$.

2.3 Titration experiments of 1

Probe **1** was dissolved in ethanol to afford a concentration of 1.0 mM stock solution, which was then diluted to 2×10^{-4} M. The tetrabutylammonium cyanide was dissolved in Tris-HCl buffer to

afford a concentration of 1.0 mM stock solution and then diluted to 10^{-4} M. In the titration experiments, we prepared a number of new solutions to afford the titration spectra, in which each curve corresponds to an independent new solution. In this way we could ensure the real concentration of probe **1** unchanged. The exact procedure was as follows: took 0.1 ml probe **1** solution of 2×10^{-4} M to a centrifuge tube, and added 1.5 ml ethanol to it. Then a certain amount (such as x ml) of TBA cyanide solution of 10^{-4} M and (2.4-x) ml Tris-HCl buffer was added. Finally, a solution of EtOH:Tris-HCl buffer=4:6 (v/v) was used to adjust the total volume to 4.0 ml. Changes in the fluorescence intensity and absorption were recorded using a fluorescence spectrometer ($\lambda_{\text{ex}} = 345$ nm, $\lambda_{\text{em}} = 445$ nm, slits: 5 nm/2.5 nm) and a UV-visible spectrophotometer, respectively.

2.4 Test strips measurement

The test strips were prepared by immersing TLC plates (3×1 cm²) in the EtOH solution of probe **1** (1.0 mM) and dried in air. Then they were deposited to various solutions of anions (1.0 mM) individually.

3 Results and discussion

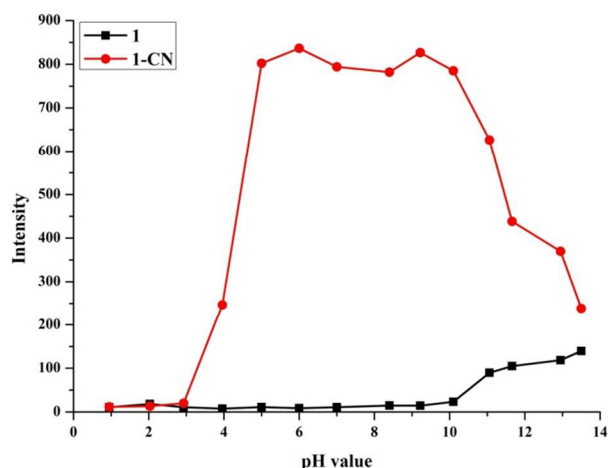


Fig.1. Fluorescence intensity at 445nm of probe **1** (5.0 μM) in EtOH-H₂O (4:6,v/v) in the absence and presence of CN⁻ measured as a function of PH. PH value were adjusted by the dilute solutions of NaOH and HCl, respectively. $\lambda_{\text{ex}} = 345$ nm, slits: 5 nm/2.5 nm.

3.1 PH dependence of 1

We first investigated the effect of pH on the fluorescence spectra of probe **1** (5.0 μM). From Fig. 1 we could find that the fluorescence intensity showed no apparent changes at pH values below 3, regardless of the absence and presence of CN⁻. This indicated that almost no reaction occurred between **1** and CN⁻. And it could be ascribed to the protonation of CN⁻ decreasing the actual concentration of CN⁻ in the sample solution. Between pH 5 and 10, **1** kept stable and responded stably to CN⁻. However, at pH higher than 10, the fluorescent intensity of **1-CN** decreased significantly. This could be attributed to the nucleophilic attack by OH⁻ to **1**. The results indicate that **1** could be used to detect CN⁻ at a range of pH values (pH = 5 - 10). Considering the environmental and biological applications, we chose the pH to be

7.4 for the testing system.

3.2 Absorption response of probe 1

The changes of the absorption spectra of **1** upon titration with CN^- in an EtOH-Tris-HCl buffer solution (10.0 mM, PH = 7.4, 4:6, v/v) were recorded. As shown in Fig. 2, probe **1** exhibited a main absorption peak at 532 nm, which was ascribed to the typical intramolecular charge transfer (ICT) band of the triphenylamine-hemicyanine dye. With the increasing of CN^- , the absorbance gradually decreased with a new peak appearing at 345 nm until saturation after titration with 3.0 equiv. of CN^- .

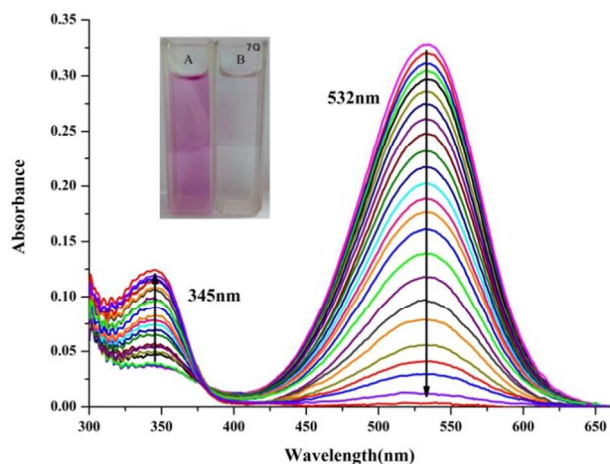


Fig. 2. Changes in absorption spectra of **1** (5.0 μM) measured in EtOH-Tris-HCl buffer (10.0 mM, pH = 7.4, 4:6, v/v) upon addition of CN^- . Inset shows the color changing of probe **1** (5.0 μM) in the absence and presence of CN^- (A: probe **1**, B: probe **1** with CN^-).

Simultaneously, an obvious color change from purple to colorless was clearly observed, suggesting that the ICT was turned off due to the nucleophilic attack of CN^- toward the indolium group of **1**. Moreover, the plot of $(1-A/A_0)$, where A_0 and A were the respective absorbance at 532 nm in the absence and presence of CN^- , vs. the concentration was found to be almost linear when the concentration of CN^- was in the range of 2.5 - 11.5 μM (Fig. S7). And we found a large color change with the CN^- inducing from Fig. S8. Therefore, this probe could be potentially used as a colorimetric probe for CN^- detection.

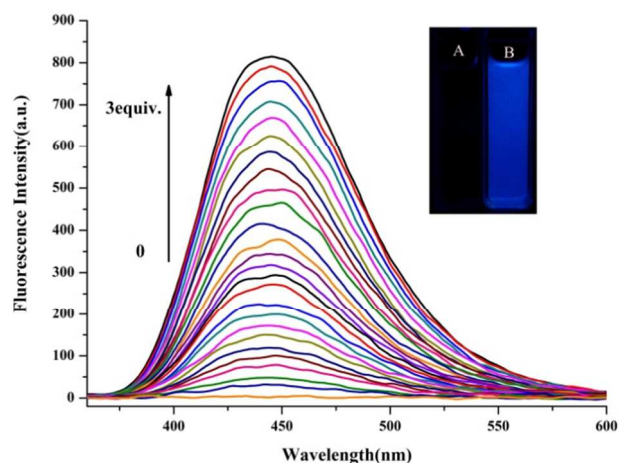


Fig. 3. Fluorescence spectra of **1** (5.0 μM) in the presence of different amounts of CN^- (from 0 to 17.0 μM) in EtOH-Tris-HCl buffer (10.0 mM, pH = 7.4, 4:6, v/v); the inset shows photos of the solution of **1** (5.0 μM) in the absence (A) or presence (B) of CN^- (15.0 μM) under UV light (365 nm). $\lambda_{\text{ex}}=345$ nm, slits: 5 nm/2.5 nm.

3.3 Fluorescence spectral titration of probe 1 toward CN^-

Fig. 3A shows the fluorescence titration of probe **1** (5.0 μM) by different amounts of CN^- (0 - 17.0 μM). The solution of probe **1** was almost non-emissive in the absence of cyanide. Upon addition of CN^- , the fluorescence intensity at 445 nm increased gradually. For instance, the fluorescence intensity increased by almost 80 times when the concentration of CN^- reached 15.0 μM (Fig. 4A). And a visual fluorescence change from colorless to blue took place synchronously (Fig. S8).

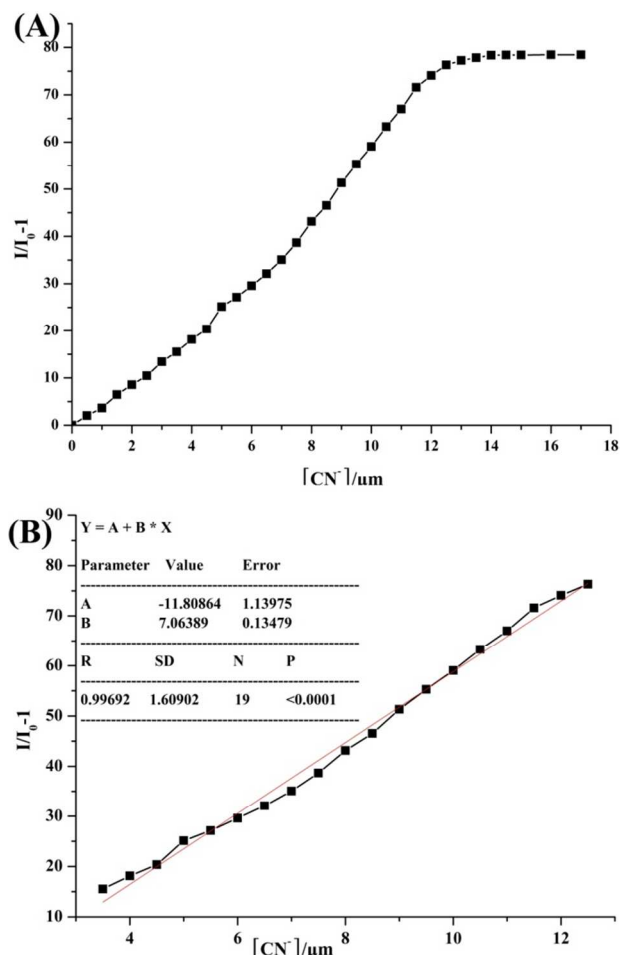


Fig. 4. (A) (I/I_0-1) plots of probe **1** (5.0 μM) at 445 nm vs. the concentration of CN^- , where I_0 and I refer to the fluorescence intensity of aqueous solution for **1** at 445 nm in the absence and presence of CN^- , respectively; (B) The linear relation between (I/I_0-1) and the CN^- concentration in the range of 3.5 - 12.5 μM .

The limit of detection (LOD) for probe **1** was also calculated based on the fluorescence titration. To determine the S/N ratio, the fluorescence intensity of **1** without CN^- was measured by 10 times and the standard deviation of blank measurements was determined to be 0.049. Under the present conditions, (I/I_0-1) varies almost linearly vs. the concentration of CN^- in the range of 3.5 - 12.5 μM , with the coefficient $R = 0.99692$ as shown in Fig.

4B. The limit of detection was then calculated with the equation³¹: $LOD = 3\sigma_{bi}/m$, where σ_{bi} is the standard deviation of blank measurements, m is the slope between $[I/I_0 - 1]$ versus sample concentration. The limit of detection was measured to be 21 nM. This indicates that probe **1** was a highly sensitive fluorescent probe for cyanide anions.

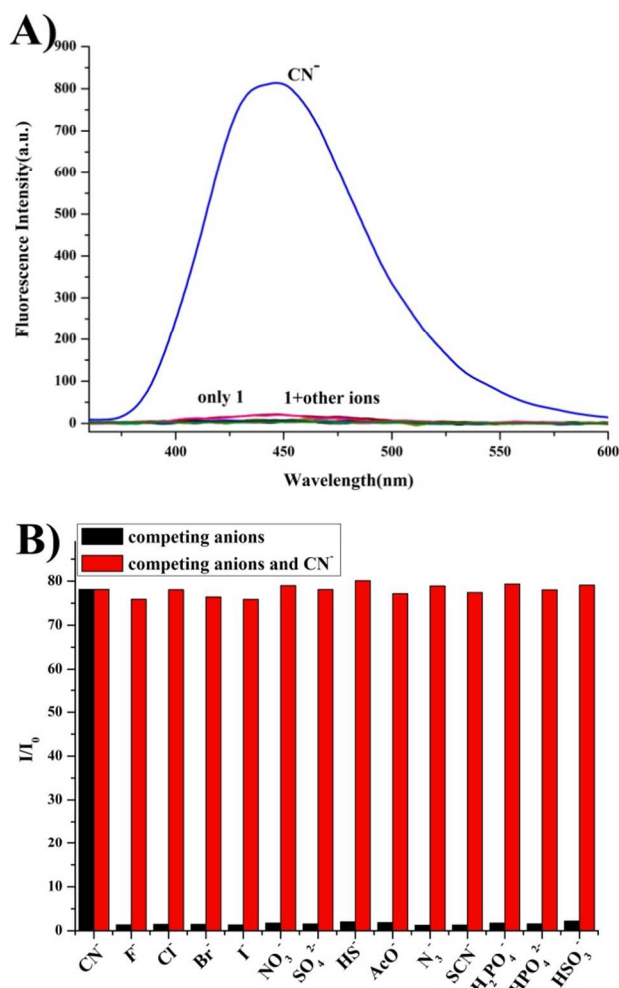


Fig. 5. A): Fluorescence spectra of **1** (5.0 μ M) with various anions in EtOH-Tris-HCl buffer (10 mM, pH = 7.4, 4:6, v/v). B): Variation of the relative fluorescence intensity at 445nm of probe **1** (5.0 μ M) in the presence of competitive anions (F⁻, Cl⁻, Br⁻, I⁻, NO₃⁻, SO₄²⁻, HS⁻, AcO⁻, N₃⁻, SCN⁻, H₂PO₄⁻, HPO₄²⁻, HSO₃⁻) and the fluorescence ratios of probe **1** (5.0 μ M) to CN⁻ (3.0 equiv.) in the presence of 30 equiv. of other competitive analytes. Insert: black bar: **1**+anion, red bar: **1**+anion+CN⁻. λ_{ex} = 345 nm, slits: 5 nm/2.5 nm.

3.4 Selectivity investigation

Another important feature of probe **1** was its high selectivity toward CN⁻ over the other competitive anions. Changes in the absorption spectra and fluorescence spectra of **1** (5.0 μ M) were measured after addition of CN⁻ and competitive species (including F⁻, Cl⁻, Br⁻, I⁻, NO₃⁻, SO₄²⁻, HS⁻, AcO⁻, N₃⁻, SCN⁻, H₂PO₄⁻, HPO₄²⁻ and HSO₃⁻) in EtOH-Tris-HCl buffer (10.0 mM, pH = 7.4, 4:6, v/v). As depicted in Fig. S9 and Fig. 5A, only addition of CN⁻ resulted in significant UV-vis spectra change and large fluorescence enhancement. Meanwhile, “naked-eye” color changes occurred. In contrast, other anions did not show any

apparent interference (Fig. S10).

Moreover, detection of CN⁻ was also examined in the presence of competitive anions. The results showed that recognizable fluorescence signal changes could be still observed after subsequent addition of CN⁻ to the probe **1** solutions in the presence of various anions, indicating that detection of CN⁻ using probe **1** in the presence of these interfering anions was still efficacious (Fig. 5B). Furthermore, the alteration of fluorescence intensity of **1** was negligible after addition of different metal ions as described in Fig. S11. Thus, all these investigations indicate that probe **1** was of highly selectivity for CN⁻.

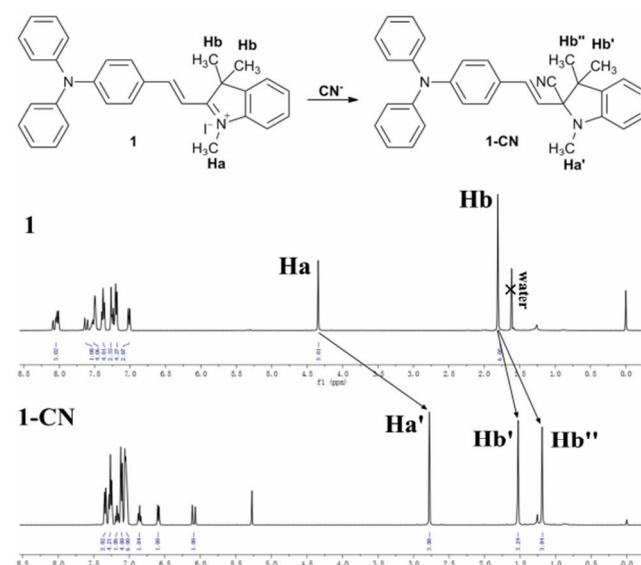


Fig. 6. The ¹H NMR spectra of probe **1** and **1-CN**.

3.5 Cyanide binding studies of **1**

As illustrated in Scheme 1, the sensing mechanism could be reasonably explained by the nucleophilic addition reaction of cyanide anion with the polarized C=N bond of the indolium group. ¹H NMR spectra was used to examine it. Fig. 6 depicts the ¹H NMR spectra of **1** before and after the addition of CN⁻. Obviously, upon addition of CN⁻, all of the ¹H NMR signals were up-field shifted. For example, the N-methyl protons (Ha) displayed an up-field shift from 4.34 ppm (3H, Ha) to 2.78 ppm (3H, Ha'). Meanwhile, the singlet peak corresponding to protons in the two CH₃ groups in probe **1** shifted from 1.81 ppm (6H, Hb) to 1.53 ppm (3H, Hb') and 1.19 ppm (3H, Hb''), forming two set of singlet peaks. This observation clearly suggested the nucleophilic attack of cyanide anion to the indolium group of probe **1** and formation of the **1-CN** adduct, in which the electron-withdrawing character of the indolium group was weakened, and as a consequence, up-field shifts generated. The Job's plot (Fig. S13) evaluated from the fluorescence spectra also proved the 1:1 binding stoichiometry between probe **1** and CN⁻. In addition, the **1-CN** adduct could be separated successfully, and ¹H NMR, ¹³C NMR, HRMS analysis further confirmed the structure. (Fig. S2, Fig. S3 and Fig. S6)

3.6 Theoretical Calculations

To gain further insight into the mechanism of the color fading and fluorescence enhancement of **1** in the presence of CN⁻,

density functional theory (DFT) calculations were carried out at the B3LYP/6-31G(d) level using the Gaussian 09 program package.³² The optimized structures of **1** and **1-CN** are shown in Fig. S14. As to **1**, the indolium group was nearly coplanar with the phenyl unit via a conjugated bridge (–C=C–), the dihedral angle between them was 177.6°. Upon interaction of **1** with CN[–], the coplanation was inhibited, and the dihedral angle between the indole and phenyl groups of **1-CN** changed to 91.8°. This structural difference gives rise to the significant difference in π -conjugation between **1** and **1-CN**.

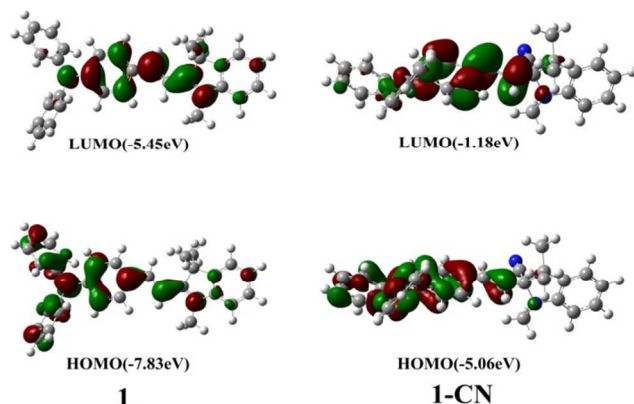


Fig. 7. The Calculated HOMOs and LUMOs distribution of **1** and **1-CN**.

Detailed information about the changes upon formation of **1-CN** could be obtained from time-dependent DFT (TD-DFT) calculations as well. The calculated molecular orbitals are shown in Fig. 7, HOMO of **1** was delocalized mainly onto the triphenylamine unit while LUMO delocalized over the phenyl and indolium groups. In contrast, both the HOMO and LUMO of **1-CN** were localized to only the triphenylamine unit. Therefore, the decreased fluorescence intensity of **1** could be attributed to ICT from triphenylamine unit to the indolium group. Nucleophilic addition of cyanide to the indolium group prevented ICT from occurring, resulting in an enhanced fluorescence emission from the triphenylamine unit.

The calculated results of transitions with oscillator strength above 0.1 are summarized in Fig. S15. The calculated absorption wavelengths of **1** and **1-CN** were 526 nm and 357 nm, respectively, with oscillator strengths of 1.3456 and 0.7646. TD-DFT calculations showed one transition at 486 nm with an oscillator strength of $f=0.0559$ which corresponded to a HOMO-LUMO transition. The calculations consistent highly with the experimental results, yet wavelength values are slightly overestimated.



Fig. 8. Fluorescence microscope imaging of live GES cells with probe **1** (20.0 μM) before (b) and after (c) treated with CN[–] (50.0 μM) for 30 minutes. Bright-field transmission imaging of GES cells was shown in (a).

3.7 Application

In order to demonstrate the practical application of probe **1** for

the detection of CN[–], the test strips were prepared to determine the suitability of a “dip-stick” method. After being immersed to the aqueous solution of CN[–], the plate’s color changed from purple to colorless quickly. However, color variation was not detected for the plates after interaction with aqueous solutions containing other anions (including F[–], Cl[–], Br[–], I[–], NO₃[–], SO₄^{2–}, HS[–], AcO[–], N₃[–], SCN[–], H₂PO₄[–], HPO₄^{2–}, HSO₃[–]) as depicted in Fig. S12. This phenomenon demonstrated that probe **1** could be used for the rapid detection of CN[–].

Probe **1** was then used for the imaging of CN[–] in cells to explore its potential biological application. The living GES cells (human breast cancer cells) were first incubated with probe **1** (20.0 μM) for 30 minutes at 37°C in 5% CO₂ atmosphere, then washed with phosphate buffered saline (PBS, pH = 7.4) three times to remove residual dye from the cells, and induced the CN[–] (50.0 μM) into the solution for another 30 minutes. The fluorescence images revealed GES cells loaded with probe **1** (20.0 μM) showed weak intracellular fluorescence (Fig. 8b). In contrast, cells displayed bright blue intracellular fluorescence (Fig. 8c) after inducing of CN[–]. These facts implied that probe **1** had successfully immersed into the cells and could be used for imaging CN[–] in living cells. The living cell images also demonstrated it could be a useful molecular probe for studying biological processes involving CN[–] within living cells.

4 Conclusions

In summary, we have successfully developed a new colorimetric and fluorescent probe for the detection of CN[–]. The experimental results demonstrated that probe **1** displayed high sensitivity (LOD=21 nM) and selectivity for CN[–] towards other anions. The sensing mechanism was well supported by DFT/TD-DFT calculations. Moreover, the live cell imaging experiment showed it could indeed visualize the changes of intracellular CN[–] in living cells. Also, **1** could be developed as a simple paper test strip system for the rapid monitoring of CN[–]. We expect that this new probe will exploit potential applications in biological and environmental detection of cyanide in future work.

Acknowledgement

We thank the National Natural Science Foundation of China (no.21174052) and Natural Science Foundation of Jilin Province of China (no.20130101024JC) for their generous financial support.

Notes and references

- ^a Department of Chemistry, Jilin University, Changchun 130021, P. R. China. Fax: +86-431-88499576; Tel: +86-431-88499576; E-mail: yangqb@jlu.edu.cn.
^b College of Materials Science and Engineering, Jilin University of Chemical Technology, Jilin 132022, PR China. Fax: +86-432-63083094; E-mail: songyan199809@163.com.

† Electronic Supplementary Information (ESI) available: ¹H NMR, ¹³C NMR and HRMS spectra of probe **1** and **1-CN**; The plot of (1-A/A₀) at 532 nm vs. the concentration of CN[–]; Color and fluorescence changes of probe **1** with the gradual addition of CN[–]. Color and fluorescence changes of probe **1** in the presence of CN[–] and other anions; Selectivity figure towards metal ions; Photograph of the TLC plates towards various anions;

Job's plot of probe 1 and CN⁻; DFT/TD-DFT calculated results. See DOI: 10.1039/b000000x/

1. (a) V. Amendola, D. Esteban-Gomez, L. Fabbrizzi and M. Licchelli, *Acc. Chem. Res.*, 2006, **39**, 343-353; (b) M. E. Jun, B. Roy and K. H. Ahn, *Chem. Commun.*, 2011, **47**, 7583-7601; (c) L. E. Santos-Figueroa, M. E. Moragues, E. Climent, A. Agostini, R. Martinez-Manez and F. Sancenon, *Chem. Soc. Rev.*, 2013, **42**, 3489-3613; (d) P. A. Gale, N. Busschaert, C. J. E. Haynes, L. E. Karagiannidis and I. L. Kirby, *Chem. Soc. Rev.*, 2014, **43**, 205-241.
2. (a) G. C. Miller and C. A. Pritsos, *Cyanide: Soc., Ind. Econ. Aspects, Proc. Symp. Annu. Meet. TMS*, 2001, pp: 73-81; (b) K. Kulig, *Cyanide Toxicity*, U. S. Department of Health and Human Services: Atlanta, GA, 1991;
3. (a) C. Baird and M. Cann, *Environmental Chemistry*, Freeman, New York, 2005; (b) B. Vennesland, E. E. Comm, C. J. Knowlles, J. Westly and F. Wissing, *Cyanide in Biology*, Academic Press, London, 1981.
4. *Guidelines for Drinking-Water Quality*, World Health Organization, Geneva, 1996.
5. (a) B. Deep, N. Balasubramanian and K. S. Nagaraja, *Anal. Lett.*, 2003, **36**, 2865-2874; (b) A. T. Haj-Hussein, *Talanta*, 1997, **44**, 545-551.
6. (a) G. Ding, H. Zhou, J. Xu and X. Lu, *Chem. Commun.*, 2014, **50**, 655-657; (b) Y. G. Timofeyenko, J. J. Rosentreter and S. Mayo, *Anal. Chem.*, 2007, **79**, 251-255.
7. T. Suzuki, A. Hioiki and M. Kurahashi, *Anal. Chim. Acta*, 2003, **476**, 159-165.
8. P. J. Anzenbacher, D. S. Tyson, K. Jursikova and F. N. Castellano, *J. Am. Chem. Soc.*, 2002, **124**, 6232-6233.
9. (a) F. J. Lebeda and S. S. Deshpande, *Anal. Biochem.*, 1990, **187**, 302-309; (b) J. Ma and P. K. D Gupta, *Anal. Chim. Acta*, 2010, **673**, 117-125.
10. (a) Z. Xu, X. Chen, H. N. Kim and J. Yoon, *Chem.Soc.Rev.*, 2010, **39**, 127-137; (b) F. Wang, L. Wang, X. Chen and J. Yoon, *Chem.Soc.Rev.*, 2014, **43**, 4312-4324.
11. (a) W. Cao, X. Zheng, D. Fang and L. Jin, *Dalton Trans.*, 2014, **43**, 7298-7303; (b) M. G. D. Holaday, G. Tarafdar, B. Adinarayana, M. L. P. Reddy and A. Srinivasan, *Chem. Commun.*, 2014, **50**, 10834-10836; (c) X. Lou, Q. Zeng, Y. Zhang, Z. Wan, J. Qin and Z. Li, *J. Mater. Chem.*, 2012, **22**, 5581-5586.
12. (a) X. Chen, S. Nam, G. Kim, N. Song, Y. Jeong, I. Shin, S. K. Kim, J. Kim, S. Park and J. Yoon, *Chem. Commun.*, 2010, **46**, 8953-8955; (c) Z. Dai and E. M. Boon, *J. Am. Chem. Soc.*, 2010, **132**, 11496-11503;
13. (a) S. Seo, D. Kim, G. Jang, J. Kim and T. S. Lee, *Polymer*, 2013, **54**, 1323-1328; (b) R. Tirfoin and S. Aldridge, *Dalton Trans.*, 2013, **42**, 12836-12839.
14. (a) Y. Chung, H. Lee, and K. H. Ahn, *J. Org. Chem.*, 2006, **71**, 9470-9474; (b) S. Saha, A. Ghosh, P. Mahato, S. Mishra, S. K. Mishra, E. Suresh, S. Das, and A. Das, *Org. Lett.*, 2010, **12**, 3406-3409; (c) S. Kim, J. Y. Noh, S. J. Park, Y. J. Na, I. H. Hwang, J. Min, C. Kim and J. Kim, *RSC Adv.*, 2014, **4**, 18094-18099.
15. M. Tomasulo, S. Sortino, A. J. P. White and F. M. Raymo, *J. Org. Chem.*, 2006, **71**, 744-753.
16. (a) F. Garcia, J. M. Garcia, B. Garcia-Acosta, R. Martinez-Manez, F. Sancenon and J. Soto, *Chem. Commun.*, 2005, 2790-2792; (b) Y. Shiraiishi, S. Sumiya and T. Hirai, *Chem. Commun.*, 2011, **47**, 4953-4955.
17. (a) S. Goswami, S. Paul and A. Manna, *Dalton Trans.*, 2013, **42**, 10682-10686; (b) M. Sun, S. Wang, Q. Yang, X. Fei, Y. Li and Y. Li, *RSC Adv.*, 2014, **4**, 8295-8299.
18. (a) S. H. Mashraqui, R. Betkar, M. Chandiramani, C. Estarellas and A. Frontera, *New. J. Chem.*, 2011, **35**, 57-60; (b) J. Li, J. Gao, W. Xiong, P. Li, H. Zhang, Y. Zhao and Q. Zhang, *Chem.-Asian. J.*, 2014, **9**, 121-125.
19. (a) P. Wang, Y. Yao and M. Xue, *Chem. Commun.*, 2014, **50**, 5064-5067; (b) Y.-K. Yang and J. Tae, *Org. Lett.*, 2006, **8**, 5721-5723.
20. (a) Y. Zhang, D. Li, Y. Li and J. Yu, *Chem. Sci.*, 2014, **5**, 2710-2716; (b) P. B. Pati and S. S. Zade, *RSC Adv.*, 2013, **3**, 13457-13462.
21. M. K. Bera, C. Chakraborty, P. K. Singh, C. Sahu, K. Sen, S. Maji, A. K. Das and S. Malik, *J. Mater. Chem. B*, 2014, **2**, 4733-4739.
22. (a) Y. Duan and Y. Zheng, *Talanta*, 2013, **107**, 332-337; (b) H. Niu, D. Su, X. Jiang, W. Yang, Z. Yin, J. He and J. Cheng, *Org. Biomol. Chem.*, 2008, **6**, 3038-3040.
23. (a) D. Kim, Y. Chung, M. Jun and K. H. Ahn, *J. Org. Chem.*, 2009, **74**, 4849-4854; (b) H. Miyaji, D. Kim, B. Chang, E. Park, S. Park and K. H. Ahn, *Chem. Commun.*, 2008, 753-755.
24. N. Gimeno, X. Li, J. R. Durrant and R. Vilar, *Chem.-Eur. J.*, 2008, **14**, 3006-3012.
25. (a) J. H. Lee, A. R. Jeong, I. Shin, H. Kim and J. Hong, *Org. Lett.*, 2010, **12**, 764-767; (b) S. Hong, J. Yoo, S. Kim, J. S. Kim, J. Yoon and C. Lee, *Chem. Commun.*, 2009, 189-191.
26. (a) S. S. Razi, R. Ali, P. Srivastava, M. Shahid and A. Misra, *RSC Adv.*, 2014, **4**, 22308-22317; (b) S. S. Razi, R. Ali, P. Srivastava and A. Misra, *Tetrahedron Lett.*, 2014, **55**, 1052-1056; (c) S. S. Razi, R. Ali, P. Srivastava and A. Misra, *Tetrahedron Lett.*, 2014, **55**, 2936-2941.
27. C. Zhou, M. Sun, C. Yan, Q. Yang, Y. Li and Y. Song, *Sens. Actuators B*, 2014, **203**, 382-387.
28. (a) Y. Ding, T. Li, W. Zhu and Y. Xie, *Org. Biomol. Chem.*, 2012, **10**, 4201-4207; (b) H. Li, B. Li, L. Jin, Y. Kan and B. Yin, *Tetrahedron*, 2011, **67**, 7348-7353.
29. (a) M. O. Odago, D. M. Colabello and A. J. Lees, *Tetrahedron*, 2010, **66**, 7465-7471; (b) H. Niu, X. Jiang, J. He and J. Cheng, *Tetrahedron Lett.*, 2008, **49**, 6521-6524.
30. Y. Yang, B. Li and L. Zhang, *Sens. Actuators B*, 2013, **183**, 46-51.
31. Y. Sun, S. Fan, L. Duan and R. Li, *Sens. Actuators B*, 2013, **185**, 638-643.
32. M. J. Frisch, G. W. Trucks, H. B. Schlegel, G. E. Scuseria, M. A. Robb, J. R. Cheeseman, G. Scalmani, V. Barone, B. Mennucci, G. A. Petersson, H. Nakatsuji, M. Caricato, X. Li, H. P. Hratchian, A. F. Izmaylov, J. Bloino, G. Zheng, J. L. Sonnenberg, M. Hada, M. Ehara, K. Toyota, R. Fukuda, J. Hasegawa, M. Ishida, T. Nakajima, Y. Honda, O. Kitao, H. Nakai, T. Vreven, J. A. Montgomery, Jr, J. E. Peralta, F. Ogliaro, M. Bearpark, J. J. Heyd, E. Brothers, K. N. Kudin, V. N. Staroverov, R. Kobayashi, J. Normand, K. Raghavachari, A. Rendell, J. C. Burant, S. S. Iyengar, J. Tomasi, M. Cossi, N. Rega, J. M. Millam, M. Klene, J. E. Knox, J. B. Cross, V. Bakken, C. Adamo, J. Jaramillo, R. Gomperts, R. E. Stratmann, O. Yazyev, A. J. Austin, R. Cammi, C. Pomelli, J. W. Ochterski, R. L. Martin, K. Morokuma, V. G. Zakrzewski, G. A. Voth, P. Salvador, J. J. Dannenberg, S. Dapprich, A. D. Daniels, Ö. Farkas, J. B. Foresman, J. V. Ortiz, J. Cioslowski and D. J. Fox, *Gaussian 09, Revision D.01*, Gaussian, Inc., Wallingford C. T., 2009.